Supporting Information

Uzawa *et al.* 10.1073/pnas.0804033105

SI Text

Usage and Calibration of the Rapid Mixer. The apparatus is composed of the mixer and three syringes (P, Q, and R). The syringes P (5 ml), Q (25 ml), and R (5 ml) supply the sample solutions to the mixer through the holes X, Y, and Z, respectively. The rapid mixer is composed of the acrylic plate (A), the first mixing plate (B), and the second mixing block (C). The two solutions derived from the syringes P and Q through the respective holes (X and Y) are mixed within 200 μs at a T-shaped point created on the first mixing plate (B) with 200-μm thickness. The mixed solution flows inside the flow channel for a folding period of t_f. The folding period can be varied by changing the pass length between the first mixing point and the small hole on the second mixing block (C). The hole with a diameter of 0.2 mm is connected to a Teflon tube with an inner diameter of 0.17 mm and a length of 17 mm. At the second mixing point, the solution after the first mixing is mixed with a 1/6 volume of the solution from the syringe R. The solution after the second mixing flows downward for a period of t_p determined by the length of the Teflon tube into a large volume of solution (S) stirred vigorously in a beaker which is set on ice (third mixing).

The mixing efficiencies of the first and second mixing were evaluated by using a discoloration reaction of pH-sensitive bromocresol purple (BCP). The completion point of the discoloration reaction for the first mixing, which is $\approx$500 μm from the center of the T-shaped mixing point, corresponds to $\approx$200 μs at a flow line speed of 2.31 m/s. The completion of the second mixing was checked by the color of the waste solution, which ensures that the complete mixing is achieved within 3.6 ms.

Reduction of Amide Exchange Rates by Heme Incorporation. In this and previous studies we have adopted a strategy of incorporating heme into apomyoglobin to reconstitute the holoprotein to stabilize amide protons against exchange and thereby maximize the number of probes available for folding studies (1, 2). Binding of heme to the apoprotein is extremely rapid (3) and is expected to be complete in $<$10 ms under the conditions of the heme insertion experiments. At the same time, exchange of the available amide probes from the holoprotein is very slow; even the most labile amide proton probes have half-lives $>$500 s, and therefore exchange during the 5-s heme insertion step is negligibly small. As a control, experiments performed previously with a conventional quench flow apparatus (dead time of 6 ms) give the same results whether amide exchange is quenched by insertion of heme or whether measurements are made directly on the apoprotein by quenching exchange in DMSO solvent (2, 4).

Measurement of Proton Occupancy. To determine the proton occupancy (H_{obs}) for each residue at any given pulse pH, the cross-peak intensity was first calibrated to allow for variation in the protein concentration according to the following equation:

$$I_N^{\prime pH} = \frac{I_N^{pH}}{I_{methyl}^{pH}},$$

where I_N^{pH} is the cross-peak height for residue (N) in the HSQC spectrum at the given pulse pH and I_{methyl}^{pH} is the intensity of a nonexchangeable methyl resonance in a 1D ^{1}H NMR spectrum recorded on the same sample. Next, the proton occupancy (H_{obs}) at each pH was calculated by normalizing the calibrated cross-peak intensity ($I_N^{\prime pH}$) relative to the fully protonated cross-peak amplitude by using the following equation:

$$H_{obs}^{pH} = \frac{I_N^{\prime pH}}{I_N^{\prime FP}},$$

where $I_N^{\prime FP}$ is the calibrated height of the cross-peak in the fully protonated state. This ensures that H_{obs} in the fully protonated state is unity. To improve the accuracy, the fully protonated intensity was calculated as an average over a range of pulse pH values (pH 7–8) where the intensities are pH-independent. Uncertainties (standard deviation) in H_{obs} were estimated to be $\approx$5% based on the observed scatter in the pH-independent proton occupancies at pulse pH values $<$ 7.5.

Data Analysis. The proton occupancies measured as a function of pH were fit to the Hvidt equations (5, 6) using IGOR Pro (Wavemetrics). The 0.4- and 6-ms data were initially fit by floating the values of k_{op} and k_{cl} at the two refolding times. Although the quality of the data are not sufficient to allow reliable fits for k_{op} and k_{cl} (large uncertainties), it was striking that k_{op} and k_{cl} (and also the stability $K = k_{cl}/k_{op}$) are the same within the experimental uncertainties at the 0.4- and 6-ms refolding times. These results strongly suggest that k_{op} and k_{cl} are not changing significantly over the refolding time range used in our experiments. To obtain a more accurate estimate of the opening and closing kinetics, for each residue the data at 0.4 and 6 ms were fitted simultaneously by using the same values of k_{op} and k_{cl} at each refolding time.

Calculation of Limits for Highly Protected Amides. For amides in the most highly protected group S, the stability (k_{cl}/k_{op}) was estimated to be $>$100. For amides in this group, a sigmoidal decay in proton occupancy was not observed in the pH window from 7 to 11, implying that the shift of the curve from that of the free amide is $>$2 pH units. Under the assumption of an EX2 exchange mechanism, the shift corresponds to a stability $>10^2$. In addition, because exchange of amide protons in this class does not occur even at pH 10.8, k_{cl} must be greater than k_{ex} (Scheme 1), which places a lower limit on k_{cl} of $\approx$40,000 s^{-1}.

1. Jennings PA, Wright PE (1993) Formation of a molten globule intermediate early in the kinetic folding pathway of apomyoglobin. *Science* 262:892–896.
2. Nishimura C, Dyson HJ, Wright PE (2002) The apomyoglobin folding pathway revisited: Structural heterogeneity in the kinetic burst phase intermediate. *J Mol Biol* 322:483–489.
3. Hargrove MS, Barrick D, Olson JS (1996) The association rate constant for heme binding to globin is independent of protein structure. *Biochemistry* 35:11293–11299.
4. Nishimura C, Dyson HJ, Wright PE (2005) Enhanced picture of protein-folding intermediates using organic solvents in H/D exchange and quench-flow experiments. *Proc Natl Acad Sci USA* 102:4765–4770.
5. Hvidt A, Nielsen SO (1966) Hydrogen exchange in proteins. *Adv Protein Chem* 21:287–386.
6. Hvidt A (1964) A discussion of the pH dependence of the hydrogen-deuterium exchange of proteins. *C R Trav Lab Carlsberg* 34:299–317.

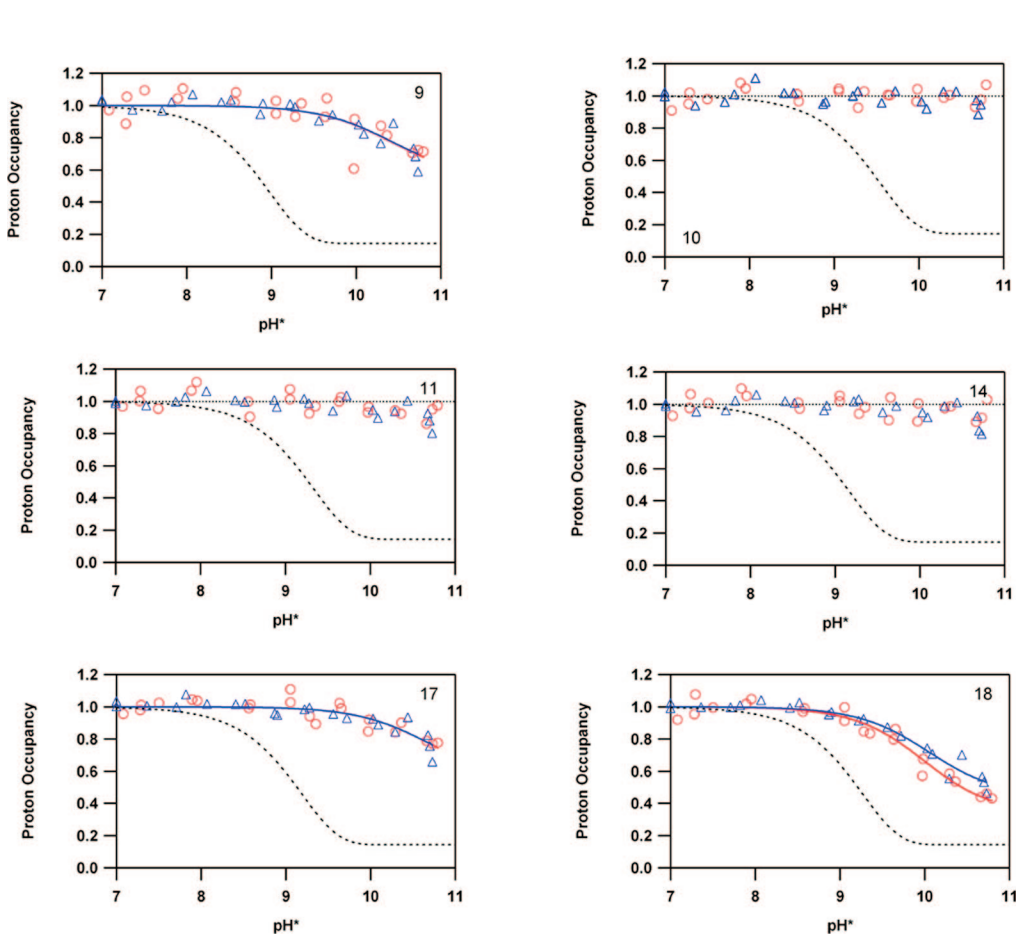

Fig. S1. Plots analogous to Fig. 2 for all probe amides of apomyoglobin.

B helix

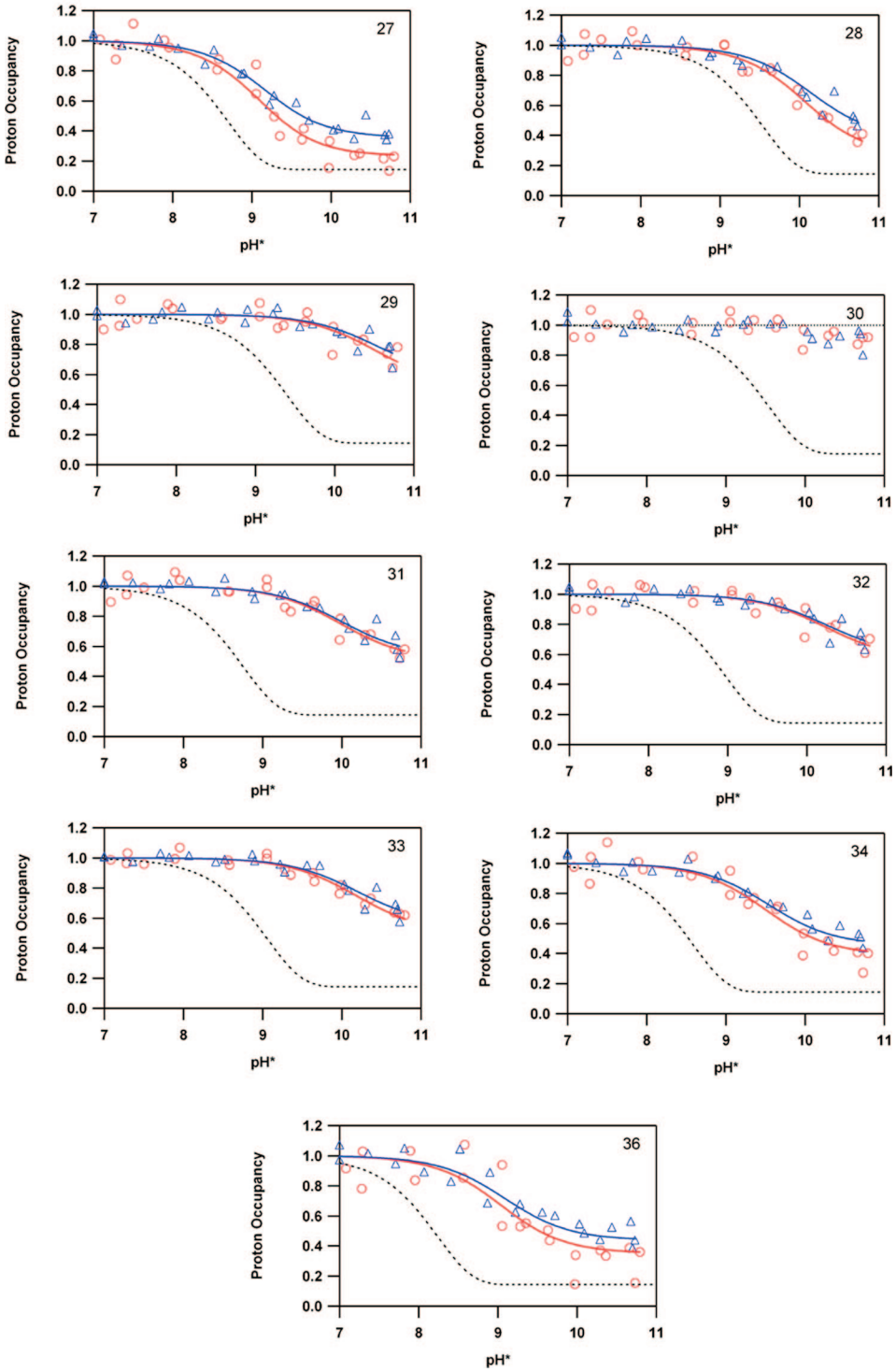

Fig. S1. (continued)

C helix, CD loop, D helix

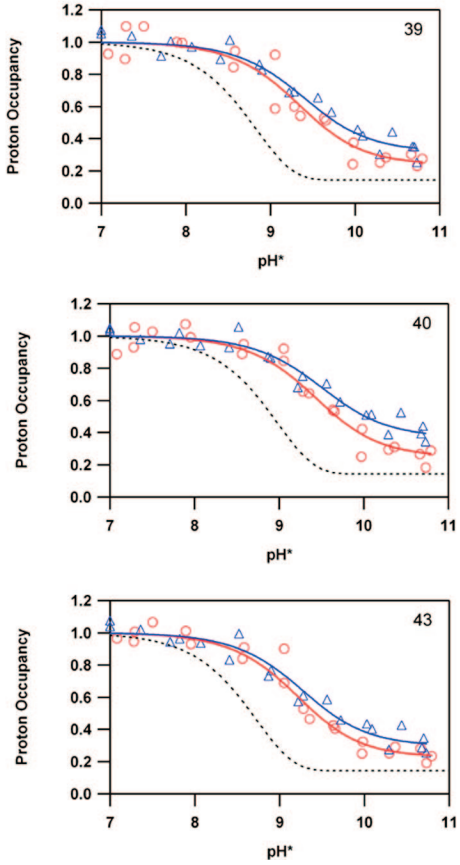

Fig. S1. (continued)

E helix

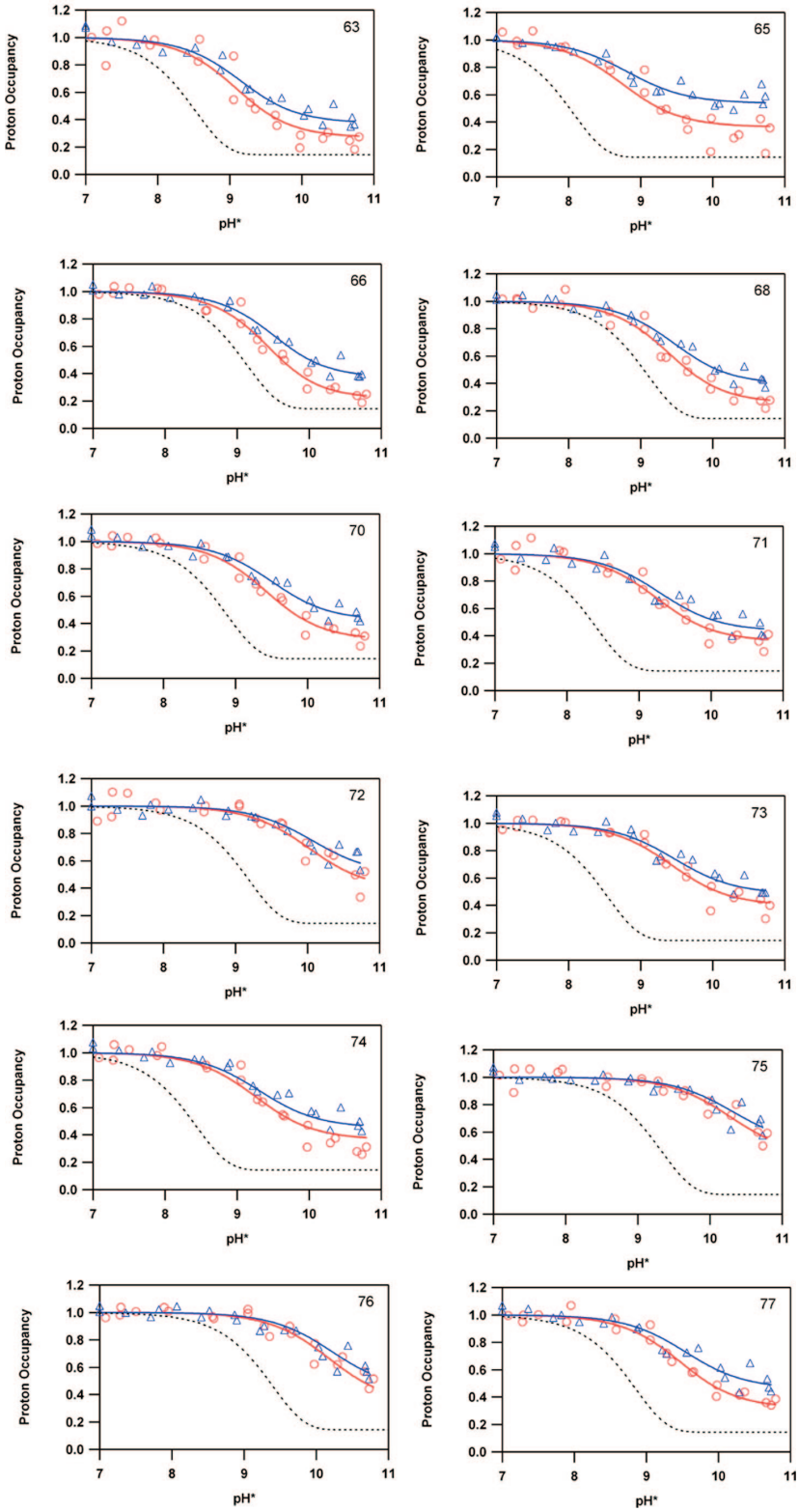

Fig. S1. (continued)

G helix

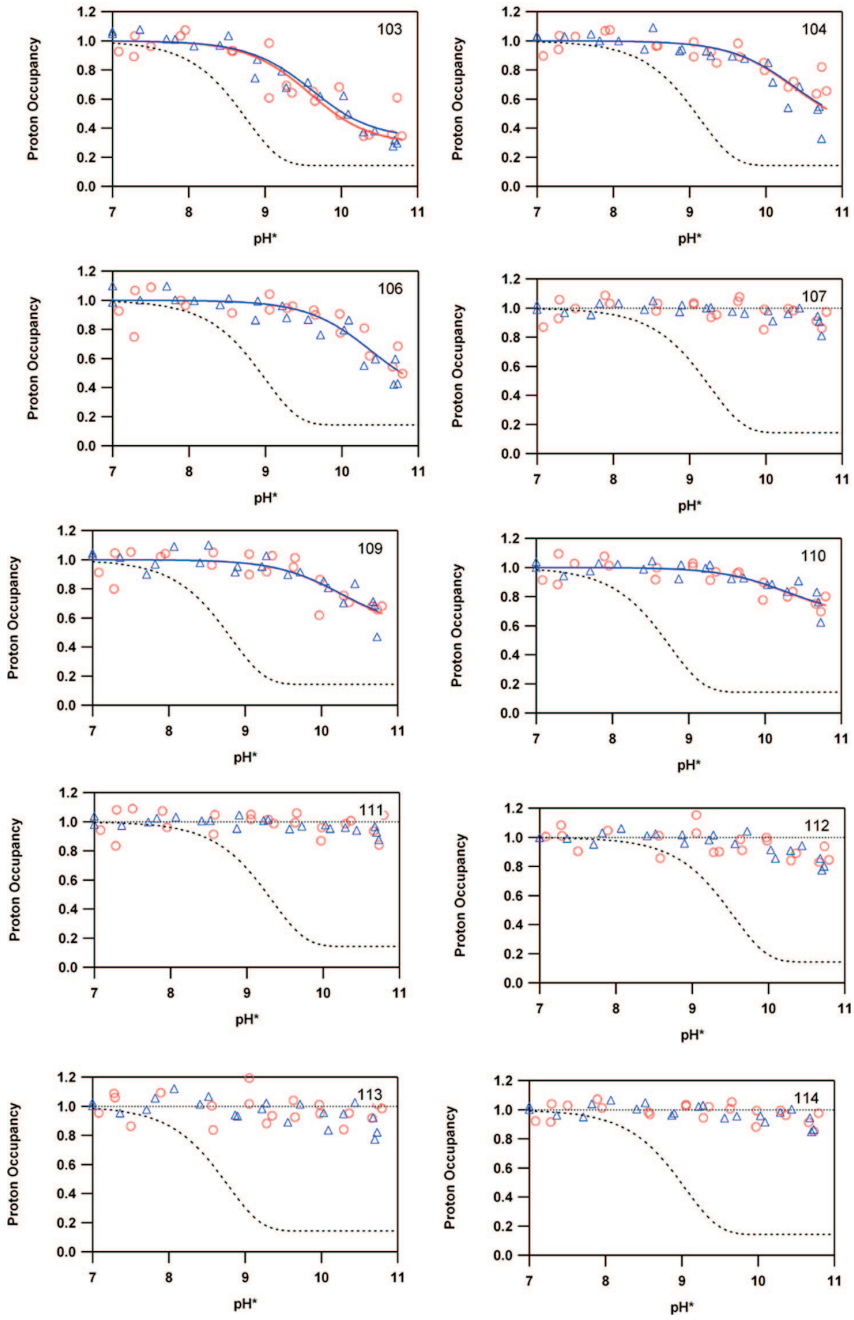

Fig. S1. (continued)

H helix

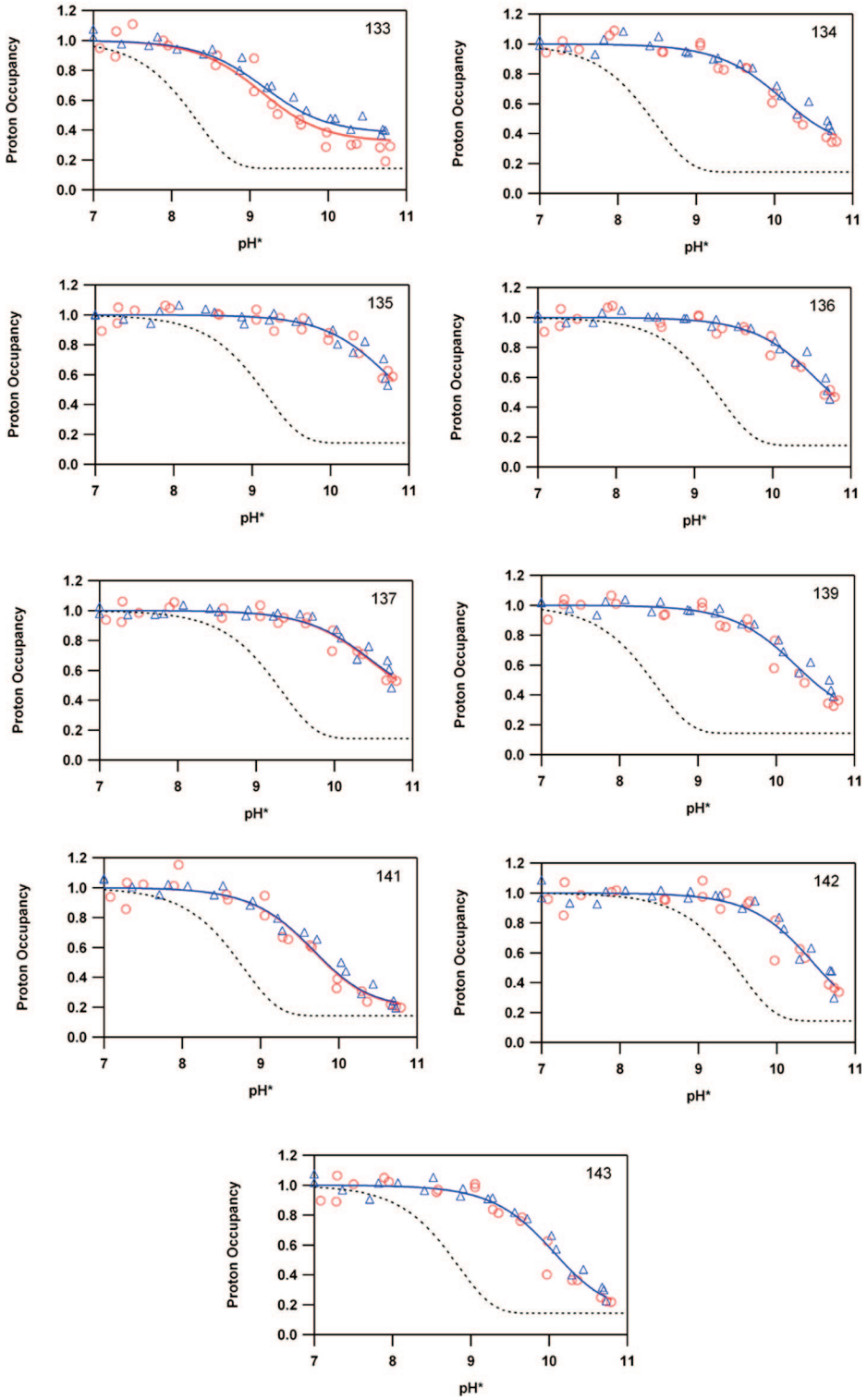

Fig. S1. (continued)

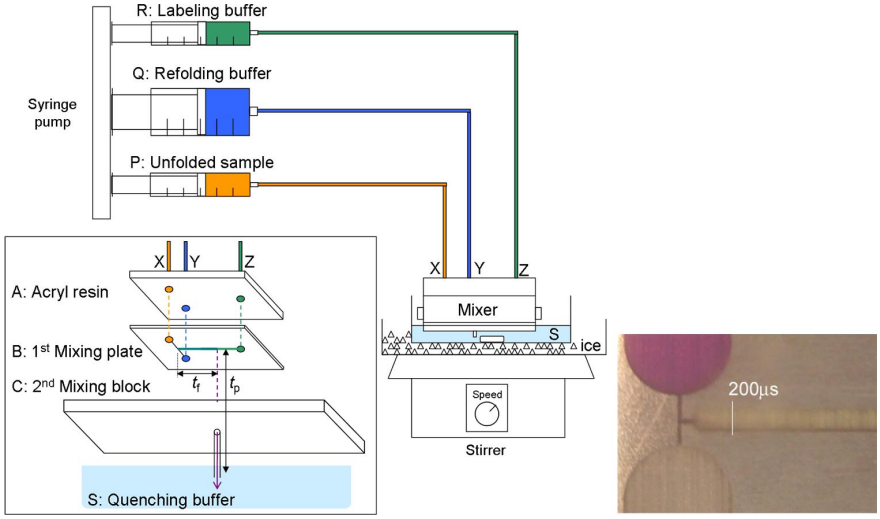

Fig. S2. (*Left*) The system developed for the rapid pulse-labeling experiments. The device is composed of the rapid solution mixer and the three syringes (P, Q, and R). The unfolded sample and refolding buffer supplied from the respective syringes (P and Q) flow in the mixer through the holes (X and Y). The two solutions are mixed at the T-shaped mixing point on the first mixing plate (B) and refolding reaction is started. The refolding solution flows to the right inside the flow channel for a period of t_f and is mixed with the pulse-labeling buffer from syringe R. The solution after the second mixing flows downward for a period of t_p and is mixed with a large volume of quenching buffer (S) stirred vigorously in the beaker and cooled on ice. (*Right*) The image of the discoloration reaction to determine the first mixing efficiency. Acetate buffer and BCP solution are flowed from the lower and upper side of the image, respectively. After the mixing at the T-shaped mixing point, the color of BCP solution changes from purple to yellow. The solutions are completely mixed within 500 μm from the mixing point, which corresponds to 200 μs at the flow speed of 2.31 m/s.

Table S1. Stability and kinetic parameters

Residue	k_{op}, s^{-1}	k_{cl}, s^{-1}	k_{cl}/k_{op}	NH_{open}, 0.4 ms	NH_{open}, 6 ms	Protection
A						
L9	200 (75)	10,000 (6,600)	53 (39)	0.03 (0.04)	0.02 (0.01)	M
V10	-	>40,000*	>100	-	-	S
L11	-	>40,000*	>100	-	-	S
W14	-	>40,000*	>100	-	-	S
V17	200 (100)	1,3000 (9,500)	61 (56)	0.02 (0.04)	0.02 (0.01)	M
E18	260 (25)	2,300 (280)	9 (1)	0.42 (0.04)	0.10 (0.01)	W
B						
D27	320 (33)	1,100 (160)	3.3 (0.6)	0.68 (0.04)	0.23 (0.03)	W
I28	300 (40)	1,500 (240)	5 (1)	0.57 (0.05)	0.17 (0.03)	W
L29	180 (52)	4,900 (1,600)	28 (12)	0.16 (0.09)	0.03 (0.01)	M
I30	-	>40,000*	>100	-	-	S
R31	210 (28)	6,500 (1,500)	31 (8)	0.10 (0.05)	0.03 (0.01)	M
L32	170 (34)	6,900 (2,100)	40 (14)	0.08 (0.05)	0.02 (0.01)	M
F33	190 (23)	5,000 (810)	26 (5)	0.16 (0.04)	0.04 (0.01)	M
K34	260 (27)	3,600 (580)	14 (3)	0.27 (0.05)	0.07 (0.01)	W
C and CD						
H36	270 (40)	2,800 (680)	10 (3)	0.36 (0.09)	0.09 (0.02)	W
T39	380 (44)	1,600 (250)	4.1 (0.9)	0.56 (0.05)	0.19 (0.02)	W
L40	310 (31)	1,200 (170)	4.0 (0.7)	0.63 (0.04)	0.20 (0.03)	W
F43	420 (43)	1,600 (250)	3.8 (0.7)	0.57 (0.05)	0.21 (0.03)	W
E						
K63	320 (35)	1,700 (290)	5 (1)	0.54 (0.06)	0.16 (0.03)	W
G65	190 (18)	1,800 (250)	10 (2)	0.49 (0.05)	0.09 (0.01)	W
V66	280 (25)	730 (86)	2.6 (0.4)	0.76 (0.02)	0.28 (0.03)	W
V68	290 (23)	1,200 (140)	4.4 (0.6)	0.63 (0.03)	0.19 (0.02)	W
T70	260 (21)	1,400 (150)	5.4 (0.7)	0.58 (0.03)	0.16 (0.02)	W
A71	280 (24)	3,100 (430)	11 (2)	0.32 (0.05)	0.08 (0.01)	W
L72	220 (32)	2,800 (480)	13 (3)	0.35 (0.06)	0.07 (0.02)	W
G73	240 (20)	3,200 (400)	14 (2)	0.31 (0.04)	0.07 (0.01)	W
A74	260 (23)	2,900 (390)	11 (2)	0.35 (0.05)	0.08 (0.01)	W
I75	230 (39)	3,700 (760)	16 (4)	0.25 (0.07)	0.06 (0.01)	M
L76	270 (40)	2,600 (460)	10 (2)	0.38 (0.06)	0.09 (0.02)	W
K77	240 (20)	1,800 (190)	7 (1)	0.52 (0.04)	0.12 (0.01)	W
G						
Y103	400 (65)	3,500 (920)	9 (3)	0.29 (0.09)	0.10 (0.03)	W
L104	350 (120)	8,000 (4,400)	23 (15)	0.07 (0.08)	0.04 (0.03)	M
F106	430 (170)	13,000 (8,500)	31 (23)	0.04 (0.04)	0.03 (0.02)	M
I107	-	>40,000*	>100	-	-	S
E109	210 (62)	11,000 (5,800)	50 (31)	0.03 (0.04)	0.02 (0.01)	M
A110	130 (35)	11,000 (5,700)	86 (49)	0.02 (0.03)	0.01 (0.01)	S
I111	-	>40,000*	>100	-	-	S
I112†	-	>40,000*	>100	-	-	S
H113	-	>40,000*	>100	-	-	S
V114†	-	>40,000*	>100	-	-	S
L115†	-	>40,000*	>100	-	-	S
H						
K133	330 (29)	3,200 (470)	10 (2)	0.32 (0.05)	0.09 (0.01)	W
A134	500 (70)	26,000 (6,200)	51 (14)	0.02 (0.01)	0.02 (0.01)	M
L135	650 (410)	26,000 (21,000)	40 (40)	0.02 (0.02)	0.02 (0.02)	M
E136	720 (290)	14,000 (7,000)	19 (12)	0.05 (0.04)	0.05 (0.03)	M
L137	380 (94)	6,900 (2,400)	18 (8)	0.10 (0.07)	0.05 (0.02)	M
F138†	-	>40,000*	>100	-	-	S
R139	680 (140)	47,000 (15,000)	70 (27)	0.01 (0.01)	0.01 (0.01)	M
D141	760 (120)	6,200 (1,400)	8 (2)	0.17 (0.05)	0.11 (0.03)	W
I142	1,200 (760)	9,500 (7,500)	8 (8)	0.12 (0.13)	0.11 (0.10)	W
A143	1,100 (290)	19,000 (6,700)	17 (8)	0.05 (0.02)	0.05 (0.02)	M

Values in parentheses represent errors estimated from the data fits. S, strong ($k_{cl}/k_{op} > 80$); M, moderate ($80 > k_{cl}/k_{op} > 15$); W, weak ($k_{cl}/k_{op} < 15$).
*No exchange observed even at pH 10.8; $k_{cl} > k_{ex} \approx 40{,}000\ s^{-1}$.
†Overlapped HSQC cross-peaks. Mutational studies show that both amides are protected in the burst phase intermediate.(1) Because there is no pH dependence of the proton occupancy, both amides must be fully protected in the 0.4- and 6-ms intermediates.

1. Nishimura C, Dyson HJ, Wright PE (2006) Identification of native and nonnative structure in kinetic folding intermediates of apomyoglobin. *J Mol Biol* 355:139–156.